A Phase-Change Random Access Memory Model for Circuit Simulation

K. C. Kwong, Philip K. T. Mok and Mansun Chan

Department of Electronic and Computer Engineering
The Hong Kong University of Science and Technology
Clear Water Bay, Kowloon, Hong Kong, China, mchan@ust.hk

ABSTRACT

A temperature tracking approach has been developed to model the behavior of phase-change memory (PCM) under input pulses with arbitrary magnitude and shapes. By utilizing the Johnson-Mehl-Avrami equation to monitor the crystal fraction in the phase-change element crystallization process, the resulting resistance of the memory is dynamically calculated. Multi-level memory program and data retention can also be simulated using the proposed method. The model has been implemented by Verilog-A and has been verified by experimental data in the literature as well as numerical simulation.

Keywords: phase-change, non-volatile memory, PCRAM

1 INTRODUCTION

Due to the potential scaling complexity of traditional flash memory cells in the nano-era, researchers are looking for alternative Non-Volatile Memory (NVM) solutions. Phase Change Memory (PCM) has emerged as one of the potential candidates due to its advantages in low power consumption, high read/write speed and excellent scalability. A lot of researches on phase-change material properties, thermal analysis of PCM cell and multi-level programming technique have been conducted. However, a complete compact model that can accurately described the behavior of PCM cells in circuit operation is still missing. Most of the published PCM models [1-5] are based on the macro-model approach, which ignores the detail effects of input pulse magnitudes and shapes. More sophisticated models [6] have also been developed, but they require the solution of implicit differential equations that make parameter extraction difficult. In addition, all the reported models have not incorporated the recent experimental findings [7] that the transition of the phase change material from crystalline to amorphous state is highly dependent on the cooling edge profile of the programming pulse rather than the duration of programming time.

In this work, we have developed a temperature tracking approach to monitor the crystal fraction of the PC element during both SET and RESET. The model composed of simple and explicit expression for each element used to allow easy parameter extraction. In addition to basic I-V characteristics of PCM memory cell, the model also allows the simulation of multi-level programming and data retention of a PCM circuit.

2 OUTPUT CHARACTERISTICS OF PCM

The structure of the PC element assumed in this work is similar to that shown in Fig. 1. The PC element can exist in the high resistance amorphous (RESET) state or the low resistance crystalline (SET) state. The I-V characteristics of a PCM cell at both states are shown in Fig. 2.

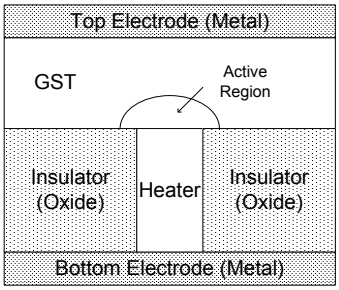

Fig. 1: PCM cell configuration with the phase change material, GST, placed between top electrode and heater

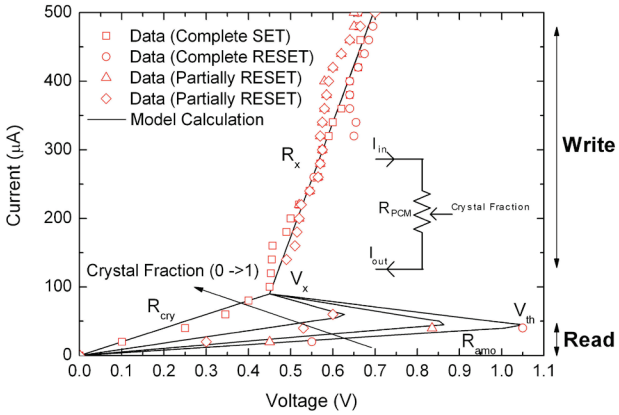

Fig. 2: Characteristics and simulation result of a PCM cell with all the characteristic parameters.

A snapback behavior is observed when a high voltage is applied to the PCM cell at the amorphous state causing a phase transition [8]. The actual resistance of the PCM cell can be somewhere in between the two extreme states depending on the crystal fraction, which assumes a value of 1 when it is fully crystallized and 0 when it is in a completely amorphous state. The resistance and threshold voltage causing phase transition have been well explained and demonstrated in [9]. They can be modeled as:

$$R_{state} = R_{amo} + C_f(t) \cdot (R_{cry} - R_{amo}) \quad (1)$$

$$V_{thstate} = V_{th} + C_f(t) \cdot (V_x - V_{th}) \quad (2)$$

R_{cry}, R_{amo}, V_{th} and V_x are parameters to be extracted from measurement that represents the crystalline state resistance, amorphous state resistance, threshold voltage to cause phase transition in the amorphous and the holding voltage after phase transition respectively as illustrated in Fig. 2. $C_f(t)$ is the crystal fraction which will be described in the next section. Fig. 3 shows the model calculation on the relationship between the PCM state resistance and threshold voltage using crystal fraction as a parameter, together with the experimental data reported in [10].

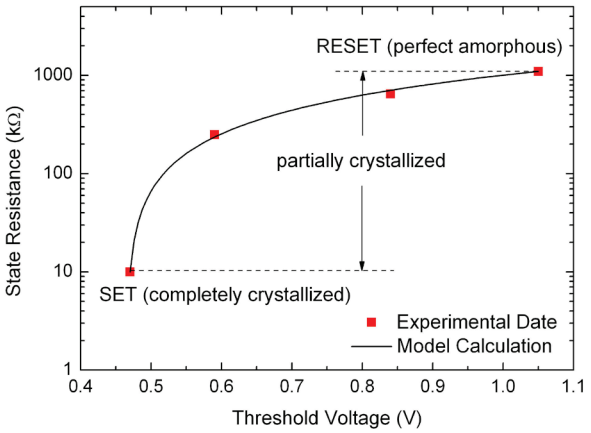

Fig. 3: Relationship between PCM cell resistance and threshold voltage during phase transition.

Based on the R_{state} and $V_{thstate}$ calculated, the resistance after snap-back (R_{tran}) can be expressed as:

$$R_{tran} = \frac{V_x - V_{thstate}}{I_x - I_{thstate}} \quad (3)$$

After deriving the resistances, voltage $V(t)$ across-the PCM cell can be expressed as a function of currents $I(t)$. However, a smooth transition between the currents and derivatives when switching from one operation region to another is necessary for the model to achieve fast convergence in a circuit simulator. A smoothing function $F(I, I_0)$ which approaches 0 when $I<I_0$ and approaches 1 when $I>I_0$ can be used to achieve the smoothing purpose, and the voltage can then be expressed as:

$$V(t) = R_{state} \cdot i_{data}(t) + R_{tran} \cdot i_{tran}(t) + R_x \cdot i_x(t) \quad (4)$$

where

$$i_{state}(t) = I(t) - F(I(t), I_{th}) \cdot [(I(t) - I_{th}]$$
$$i_{tran}(t) = F(I(t), I_{th}) \cdot [(I(t) - I_{th}] - F(I(t), I_x) \cdot [I(t) - I_x]$$
$$i_x(t) = F(I(t), I_x) \cdot [(I(t) - I_x]$$

Any mathematical function that can perform the fitting can be used as the smoothing function [4]. In this work, a Fermi-Dirac function is used to perform the function of $F(I,I_0)$ due to its simplicity. The behavior of the model is shown in Fig. 2 together with experimental data from [10]. The property of the PCM cell is well described by the crystal fraction $C_f(t)$.

3 TEMPERATURE TRACKING

The temperature history of a PCM cell is the most important factor to determine its state. The temperature variation is governed by the heat transfer equation [11]:

$$c\frac{\partial \Delta T(t)}{\partial t} = H + \nabla[k \nabla \Delta T(t)] \quad (5)$$

where ΔT is the induced temperature, H is the total heat generated, c is the heat capacitance per unit volume and κ is the thermal conductivity. The heat generation in PCM cell is caused by joule heating induced by the cell resistance when driven by a uniform input current pulse. The heat generated or power input can be expressed in term of the current $I(t)$ and resistance R of the memory element:

$$P_{in} = H = I^2(t) \cdot R \quad (6)$$

Physical quantities such as the thermal resistance and the heat capacitance are to be extracted from the measured data. At the same time, the heat generated through the programming current is dissipated to the surrounding causing a three-dimensional heat lost expressed by:

$$P_{lost} = \nabla[k \nabla \Delta T(t)] = k(\frac{\partial^2 \Delta T(t)}{\partial x^2} + \frac{\partial^2 \Delta T(t)}{\partial y^2} + \frac{\partial^2 \Delta T(t)}{\partial z^2}) \quad (7)$$

Since the insulator surrounding the PC material is has a low thermal conductance relative to the metal on the top and bottom of the structure (refer to Fig. 1), the thermal resistance in the (x-y) direction is relatively small. The heat generated is mainly dissipated along the thickness of the PCM cell where the PC material is in contact with the metal in the z-direction, which has been verified by numerical thermal simulation. The lumped thermal resistance model similar to that reported in [3] can be applied to approximate the heat lost term:

$$P_{lost} = k \cdot (\frac{V}{l}) \cdot (\frac{\Delta T(t)}{l}) \quad (8)$$

where l is the thickness and V is the volume of the phase change material. Putting (6) and (8) into (5), we obtain:

$$Vc\Delta T(t) = \int [I^2(t) \cdot R - (\frac{kV}{l^2}) \cdot \Delta T(t)] dt \quad (9)$$

Equation (9) is not solved directly, but implemented as a *RC* subcircuit as shown in Fig. 4 to facilitate circuit simulation.

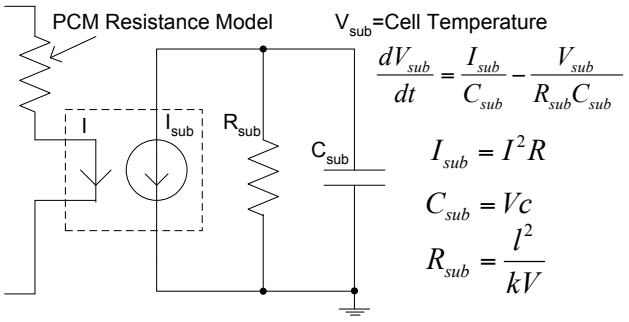

Fig. 4: Schematic of the temperature sensing subcircuit with modeling equations.

The resistor and capacitor in the *RC* subcircuit represents the thermal resistance and thermal capacitance of the device to be extracted experimentally. The *RC* subcircuit approach can also track the steady state heat flow that makes the exact location of the heat source unimportant in the simulation [12]. The output voltage of the thermal subcircuit is given by:

$$\frac{dV_{sub}}{dt} = \frac{I_{sub}}{C_{sub}} - \frac{V_{sub}}{R_{sub}C_{sub}} \tag{10}$$

By comparing equation (5) and (10), the corresponding values of the elements in the subcircuit are

$$I_{sub} = I^2R,\ C_{sub} = Vc,\ R_{sub} = \frac{l^2}{kV} \tag{11}$$

and the solution to equation (9) is given by the voltage V_{sub}.

The temperature responses of different PCM cells with extracted parameters listed in Table 1 are studied and the simulation results are shown in Fig. 5 (a). According to the simulation results, the cell C configuration has the highest cooling rate while having the same heating rate as cell D and cell E. The high cooling rate is resulted from a smaller PC material thickness. Cell E can be heated up more rapidly when compared with cell C and cell D using the same current pulse because of a low cooling rate. Also, the temperature of the cell E took a longer time to cool down after the removal of the pulse. The temperature responses of cell A, B and C are shown in Fig. 5 (b). Cell C is being heated up the fastest when compared with cell A and B, while the cooling rate of the three cells are similar. The high heating rate is resulted from the higher cell resistance. The shape of their temperature profile is the same except that cell C can be heated up to a much higher temperature. After the removal of the current pulse, the temperature of all the cells drops with similar cooling rate.

Cell	I_{sub}	R_{sub}	C_{sub}	Cooling Rate	Heating Rate
A	$(100)I^2$	58.2k	0.56p	$(30.6x10^6)V_{sub}$	$(178x10^{12})I^2$
B	$(150)I^2$	58.2k	0.56p	$(30.6x10^6)V_{sub}$	$(2.67x10^{14})I^2$
C	$(200)I^2$	58.2k	0.56p	$(30.6x10^6)V_{sub}$	$(3.56x10^{14})I^2$
D	$(200)I^2$	100.2k	0.56p	$(17.8x10^6)V_{sub}$	$(3.56x10^{14})I^2$
E	$(200)I^2$	150.2k	0.56p	$(11.9x10^6)V_{sub}$	$(3.56x10^{14})I^2$

Table 1: Cell Configurations for Temperature Simulation

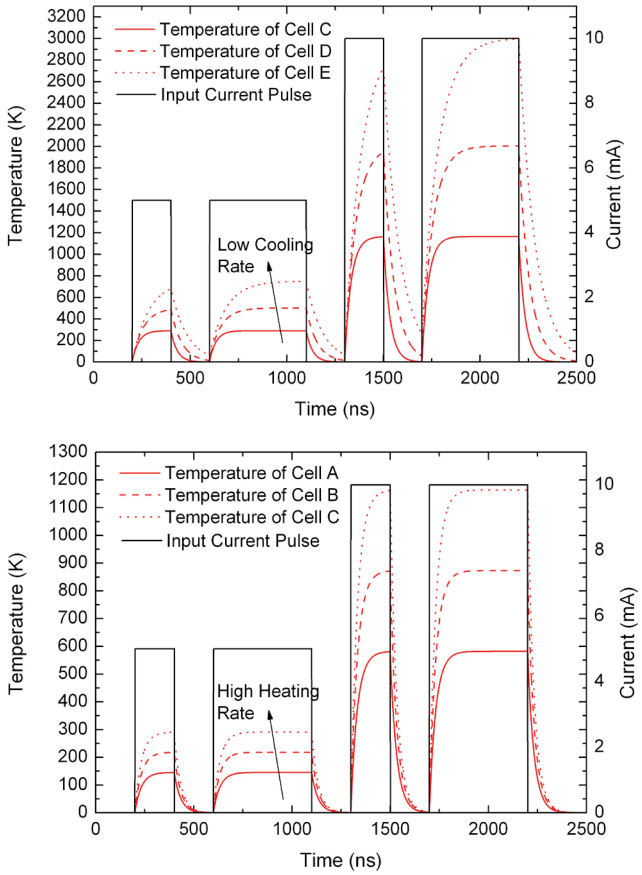

Fig. 5: Temperature response of PCM cell with (a) different cooling rates and (b) heating rate under different current input characteristics (duration and amplitude)

4 PRORAMMING

Programming of a PCM cell is achieved by raising the temperature of the cell by applying current pulses. Depending on the magnitude and duration of the pulses, a PCM cell can be SET to the crystalline state (considered to be the "1" state) or RESET to the amorphous state (considered to be the "0" state).

4.1 SET Programming

SET programming occurs when a PCM cell is heated up to a temperature below the melting point and maintained for a certain period of time to anneal and crystallize the PC material. The process can be described by the Johnson-

Mehl-Avrami (JMA) equation [13][14]. However, the original JMA equation can only be applied to constant temperature annealing. In PCM operation, the temperature is influenced by the history of heating cycle as well as the shape of the input pulse. To capture the detail in the SET operation, the JMA equation is modified to:

$$C_f(t) = 1 - e^{-K(t)\cdot t} \tag{12}$$

$$K(t) = K_0 \cdot e^{\{\frac{-E_a}{k_B\cdot[\Delta T(t)+T_{sur}]}\}} \tag{13}$$

where $K(t)$ is the crystallization time constant depending on the cell temperature, K_0 is a constant multiplier, E_a is the activation energy of the phase change material, k_B is the Boltzmann constant and T_{sur} is the temperature of the surrounding. Whenever there is a temperature change of the cell, the crystallization time constant is recalculated accordingly to reflect the changes in the cell resistance. As the temperature of the cell increases, the crystallization time constant also increases to speed up the crystallization process. At the time when the current pulse is removed, the PCM would stay at the current state with the same crystal fraction. The crystallization process will then be continued with the same crystal fraction when the next pulse is applied. A *RC* circuit as shown in Fig. 6 is used to implement the temperature dependent crystallization time constant and the crystal fraction as a state variable. The corresponding values of the components can be determined according to equation (12) and (13) which are also shown in Fig. 6. The output voltage of the circuit keeps track of the crystal fraction which is given by

$$C_f(t) = R_{SET}(t)\cdot I_{SET}(t)\cdot[1 - e^{-\frac{t}{R_{SET}(t)\cdot C_{SET}}}] \tag{14}$$

The subcircuit will automatically limit the crystal fraction to between 0 and 1 corresponding to the complete amorphous and crystalline states respectively. It should be noted that the temperature tracking circuit would also track the residual annealing generated by the read process for studying the reliability of data storage over prolong operation.

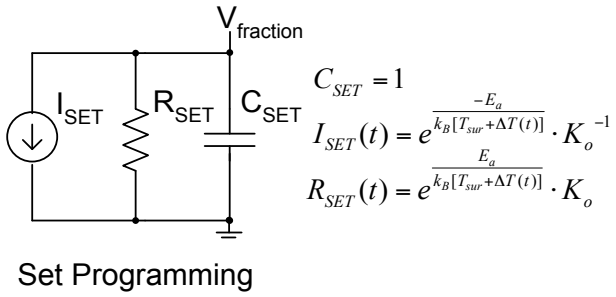

Fig. 6: Schematic of the crystal fraction calculation subcircuit for set programming with modeling equations

4.2 RESET Programming

RESET occurs when the temperature of the PCM cell increases beyond the melting point of the material. When the phase change material is heated up to its melting point by an input pulse, the material start to change phase. When the input pulse is removed, the PC element cools down to a temperature below the glass transition point. Depending on the cooling rate, the PCM cell will attain a different crystal fraction [4][11][15]. For fast cooling, the phase change material will retain an irregular atomic arrangement and form an amorphous region. In this case, the crystal fraction will be very small and approach to 0. With slower cooling rate, the temperature of the phase change material will enter the region between the melting point and glass transition point resulting in an effective annealing process. The phase-change material rearranges the atomic structure and becomes more regular, resulting in a higher crystal fraction. So, the crystal fraction of a PCM cell after RESET is less dependent on the heating process, but the cooling rate when the input pulse is removed. Some PCM models [4][5] try to account for this effect by measuring the fall time of the current pulse, which is referred as the quenching time. However, using the quenching time alone is not sufficient to model the final resistance of the PCM cell accurately as the crystal fraction is determined by the actual temperature history of the cell and not just the fall time of the current pulse. In our model, both temperature and time are taken into account by using the thermal budget, which is a product of temperature and time. The thermal budget can be calculated by

$$P(t) = \int_{t_m}^{t_g} [T_{sur} + \Delta T(t)]dt \tag{15}$$

where T_g and T_m are the glass transition point and melting point of the phase change material respectively. Based on the thermal budget that applied to anneal the crystal, the crystal fraction during cooling can be calculated by:

$$C_f(t) = [1 + e^{\frac{P_0 - P(t)}{h}}]^{-1} \tag{16}$$

where P_0 is the thermal budget to achieve half crystallization (or $C_f(t)$=0.5) and h is a parameter related to the material sensitivity to temperature change. From equation (16), the smaller the thermal budget will result in smaller crystal fraction as expected.

5 MODEL IMPLEMENTATION AND CIRCUIT SIMULATION

The described PCM model has been implemented into a SPICE engine using the Verilog-A language to perform circuit simulation and verification together with the access device and peripheral circuits. The schematic of the full

model is shown in Fig. 7 and the model parameters are listed in Table 2.

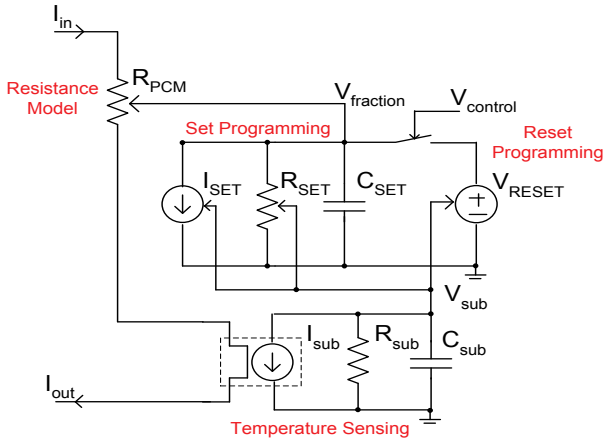

Fig. 7: Overall schematic of the PCM model. The temperature sensing circuit calculates the cell temperature for the SET and RESET programming circuit to generate the corresponding crystal fraction. The crystal fraction will then determine the I-V characteristic of the PCM cell.

Parameter	Unit	Description
Resistance Model		
R_{cry}	Ω	Crystalline (SET) resistance
R_{amo}	Ω	Amorphous (RESET) resistance
R_x	Ω	Holding resistance
V_{th}	V	Snapback voltage
V_x	V	Holding voltage
Device Structure		
l	m	Thickness of the PC material
V	m^3	Volume of the PC material
Phase Change Material Physical Property		
k	$JcmK^{-1}S^{-1}$	Thermal conductivity
c	$Jcm^{-3}K^{-1}$	Specific heat
T_g	K	Glass transition point
T_m	K	Melting point
T_{sur}	K	Surrounding Temperature
E_a	eV	Activation energy of crystallization
K_0	N/A	JMA equation constant
P_0	Ks	Thermal budget for half crystallization
h	Ks	Thermal budget sensitivity

Table 2: List of Input Parameters of the Model

When a chain of READ and WRITE input pulses is applied to the PCM cell, the corresponding output voltage, cell temperature and crystal fraction are shown in Fig. 8. The PCM cell is initially set to the amorphous state. When a small READ current is applied to the cell, the voltage output is at 0.5V due to the high amorphous state resistance. A few programming current pulse are then applied to the cell to perform SET, RESET and partial RESET. The correct behavior is observed in the READ operation predicted by the model. The programming characteristic of PCM is also calibrated with experimental data in [5] and the resulting resistance as a function of programming current is shown in Fig. 9. The model is able to track the detail of the PCM resistance at different programming current level. This property is important for simulating multi-level PCM operations.

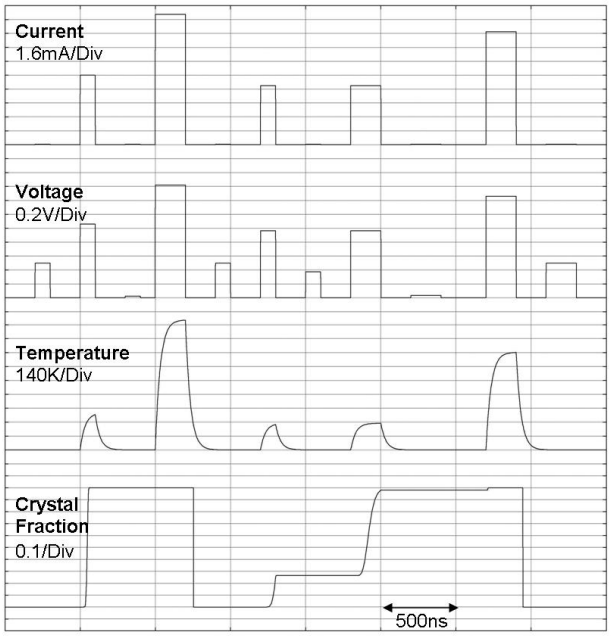

Fig. 8: Signal-time plot of the PCM simulation including current, voltage, temperature and crystal fraction

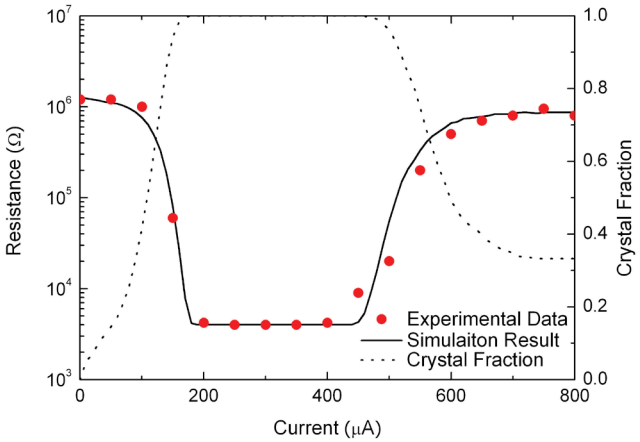

Fig. 9: Cell resistance against magnitude of applied current pulse during programing and comparison with experimental data

Data retention is one of the main concerns of non-volatile memory. The characteristics of data retention has been simulated using our model calibrate to the experimental data in [16] when the corresponding temperature is fixed at 180°C, 190°C and 210°C. Fig. 10 shows the evolution of the cell resistance with respect to time starting with the amorphous state. The simulation demonstrates the gradual RESET process at elevated temperature and the crystal fraction changes from 0 to 1. Eventually, the cell lost its RESET state due to the elevated temperature. For a higher surrounding temperature, the crystallization process of PCM occurs faster and the simulation indicates the capability of the described model to predict the data retention property of a PCM cell.

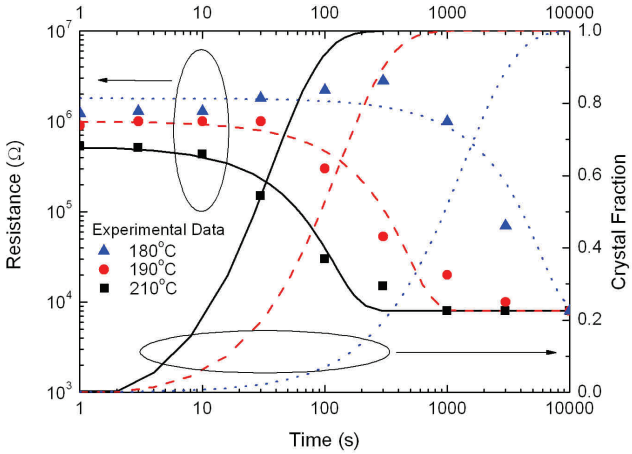

Fig. 10: Data Retention Comparison between simulation result and experimental data

6 CONCLUSION

Based on the temperature tracking approach, a physical PCM model has been developed to describe the detail of phase transition from amorphous to crystalline and crystalline to amorphous. The model has been implemented into a circuit simulator using the Verilog-A language and verified by data published in the literature. The proposed model has significantly reduced number of internal nodes for fast simulation with more enriched features.

ACKNOWLEDGEMENT

This work is jointly supported by the Area of Excellence Fund provided by the University Grant Council of Hong Kong under project number (AOE/P-04/08-1), the National High Technology Research and Development Program of China (863 program, 2008AA031402) and the Shenzhen Science & Technology Foundation (CXB201005250031A)

REFERENCES

[1] R. A. Cobley and C. D. Wright, "Parameterized SPICE model for a phase–change RAM device", IEEE, TED vol. 53, no.1, January 2006

[2] X. Q. Wei, L. P. Shi, R. Walia, T. C. Chong, R. Zhao, X. S. Miao and B. S. Quek, "HSPICE macromodel of PCRAM for binary and multilevel storage", IEEE, TED vol. 53, no. 1, January 2006

[3] Y.-B. Liao, Y.-K. Chen and M.-H. Chiang, "An analytical compact PCM model accounting for partial crystallization", IEEE, EDSSC 2007, pp. 625-628

[4] P. Fantini, A. Benvenuti, A. Pirovano, F. Pellizzer, D. Ventrice and G. Ferrari, "A compact model for phase change memories", IEEE, SISPAD 2006, pp. 162-165

[5] D. Ventrice, P. Fantini, A. Redaelli, A. Pirovano, A. Benvenuti and F. Pellizzer, "A phase change memory compact model for multilevel application", IEEE, EDL, vol. 28, no. 11, 2007

[6] K. Sonoda, A. Sakai, M. Moniwa, K. Ishikawa, O. Tsuchiya and Y. Inoue, "A compact model of phase-change memory based on rate equations of crystallization and amorphization", IEEE, TED vol. 55, no. 7, July 2008

[7] D. Mantegazza, D. Ielmini, E. Varesi, A. Pirovano, and A.L. Lacaita, "Statistical analysis and modeling of programming and retention in PCM arrays", IEEE, IEDM Technical Digest, p. 311-314, 2007

[8] A. Pirovano, A.L. Lacaita, F. Pellizzer, S. A. Kostylev, A. Benvenuti and R. Bez, "Low-field amorphous state resistance and threshold voltage drift in chalcogenide materials", IEEE, TEF, vol.51, no. 5, May 2004

[9] D. Ielmini, A. L. Lacaita and D. Mantegazza, "Recovery and drift dynamic of resistance and threshold voltages in phase-change memories", IEEE TED, vol. 54, no. 2, February, 2007

[10] A. L. Lacaita, A. Redaelli, D. Ielmini, F. Pellizzer, A. Pirovano, A. Benvenuti and R. Bez, "Electrothermal and phase-change dynamics in chalcogenide-based memories", IEEE, IEDM 2004, pp. 911-914

[11] Atlas User Manual, Silvaco

[12] S. B. Kim and H.–S. P. Wong, "Analysis of temperature in phase change memory scaling", IEEE, EDL, vol. 28, no. 8, August 2007

[13] J. Malek, "The applicability of Johnson- Mehl-Avrami model in the thermal analysis of the crystallization kinetics of glasses", Thermochimica Acta, Vol 267, pp.61-73

[14] N. Mehta, "Allications of chalcogenide glasses in electronics and optoelectronics: A review", J. of Sci. & Ind. Research, vol. 65, October 2006, pp. 777-786

[15] A. L. Lacaita and D. Ielmini, "Status and challenges of PCM modeling", IEEE, ESSDERC 2007, pp. 214-221

[16] U. Russo, D. Ielmini, A. Redaelli and A. L. Lacaita, "Intrinsic data retention in nanoscaled phase change memories-part 1: monte carlo model for crystallization and percolation", IEEE TED, vol. 53, no. 12, 2006